



# Retinal-based polyene fluorescent probe for selectively detection of $\text{Cu}^{2+}$ in physiological saline and serum

Yang Li <sup>a</sup>, Haichuang Lan <sup>a,\*</sup>, Xia Yan <sup>a</sup>, Xiaotao Shi <sup>a</sup>, Xiao Liu <sup>b</sup>, Shuzhang Xiao <sup>a,\*\*</sup>

<sup>a</sup> College of Biological and Pharmaceutical Sciences, Engineering Research Center of Eco-environment in Three Gorges Reservoir Region, Ministry of Education, China Three Gorges University, Yichang, Hubei, 443002, PR China

<sup>b</sup> Pall Corporation, 25 Harbor Dr, Port Washington, NY, 11050, USA

## ARTICLE INFO

### Article history:

Received 17 August 2019

Received in revised form

16 September 2019

Accepted 22 September 2019

Available online 20 October 2019

### Keywords:

Retinal

Fluorescence

Chemosensor

Copper cation

## ABSTRACT

Retinal is a flexible natural chromophore and widely present in organisms. The slender conjugated polyene structure retinal is conducive to entering protein structure. In this work, a novel turn-on fluorescent probe for  $\text{Cu}^{2+}$  based on retinal and phenylenediamine was designed and synthesized. The probe achieved recognition of copper ions in human serum complex protein environment. Furthermore, the high sensitivity, selectivity for  $\text{Cu}^{2+}$  and the sensing mechanism was also investigated.

© 2019 Elsevier B.V. All rights reserved.

## 1. Introduction

Retinal is a natural biochemical chromophore with conjugated polyene. There are more than 300 photochemically active proteins in the living system with retinal as their photochromic chromophore [1]. Retinal possessed innate biocompatibility, which can be widely used as the chromophore of fluorescent probes from organic solvent to a physiological environment. In recent years, significant emphasis has been placed on exploring or mimicking retinal photochemistry and photophysics in unique steric and dielectric protein environment [2–4]. However, the retinal derivatives were rarely used as a fluorescent probe due to their poor fluorescence performance [5]. In order to make full use of the fluorophore biocompatibility advantage and improve its fluorescent performance, the conjugated polyene structure of retinal was appropriately modified in this work. The modifications based on fluorescence properties have been reported [6], here we focus on the development of retinol-based copper ion fluorescent probe.

Copper ions play a critical role in the area of biological systems. As a cofactor for the enzyme, only when copper ions are bonded to proteins can they participate in physiological processes, such as cell

respiration, neurotransmission, iron uptake and defense against oxidative stresses [7]. Copper ions have also been found to be associated with many diseases, such as Alzheimer's disease [8], Parkinson's disease [9,10], prion disease [11], Wilson's disease [12] and familial amyotrophic lateral sclerosis [13]. Therefore, it is very important to develop highly selective, sensitive and rapid probe for  $\text{Cu}^{2+}$ . However, the protein environment in which copper ions are located increases the difficulty of detecting copper ions. Generally, fluorescent probes employ larger conjugated chromophores, which are not conducive to entering protein structure. Comparatively, the flexible conjugated polyene structure retinal chromophore provides a possibility to solve the problem.

Fluorescent 'turn-on' probes have been highly regarded due to their high sensitivity, selectivity and ease of observation [14–18]. Among many kinds of signaling mechanisms for optical detection of  $\text{Cu}^{2+}$ , the organic fluorescent molecules with Schiff base structure was selected in this work due to their rapid response, high sensitivity, and excellent selectivity [19–23]. However, conjugated structures with multiple aromatic rings are inherently poorly soluble, the probes will become less soluble when coupled with the Schiff base structure [24]. The construction of probes based on flexible fluorophores is an ideal choice. The luminescent properties of the flexible fluorescent probe before the binding of copper ions are poor. Once the copper ion and the probe are bound, the probe structure becomes rigid, the conjugation is stable and the luminescent properties are greatly enhanced. Among many fluorophores, retinal is an ideal candidate [25].

\* Corresponding author.

\*\* Corresponding author.

E-mail addresses: [haichuanglan@ctgu.edu.cn](mailto:haichuanglan@ctgu.edu.cn) (H. Lan), [shuzhangxiao@ctgu.edu.cn](mailto:shuzhangxiao@ctgu.edu.cn) (S. Xiao).

The soft retinal chromophore backbone without functional substituents is not suitable for binding copper ions [26]. Previously, we developed a fluorescent probe for  $\text{Cu}^{2+}$  based on *o*-phenylenediamino [24] as chelator, which exhibited excellent selectivity. In this work, a novel fluorescent probe was designed and synthesized, the *o*-phenylenediamino as a Schiff base chelator, the retinal as the reporter. The probe with Schiff base actually still has good solubility, due to the soft chromophore retinal. As expected, the soft probe becomes rigid in the process of sensing copper ions, promoting significant changes in the fluorescence.

## 2. Experimental

### 2.1. Reagents

Retinol acetate,  $\text{MnO}_2$ , *o*-Phenylenediamine were purchased from J&K Chemical Ltd. Tetrahydrofuran, ethyl acetate, acetonitrile, metal ions purchased from Sinopharm Chemical Reagent Co., Ltd. (Shanghai). Human serum was from Solarbio. Other chemicals were provided from Sigma-Aldrich. All commercially purchased chemical reagent materials were used without further purification.

### 2.2. General method

$^1\text{H}$  NMR (400MHz) and  $^{13}\text{C}$  NMR (100MHz) spectra data were recorded on a Bruker UltrashieldTM 400MHz Plus nuclear magnetic resonance spectrometer using  $\text{DMSO-}d_6/\text{CDCl}_3$  as solvent and tetramethylsilane as an internal standard. High-resolution mass spectra were carried out on a Bruker Micro TOF II 10257 instrument. Fourier transform infrared (FT-IR) spectra were performed by using NICOLET NEXUS 470 spectrometer (KBr discs) in the 4000–400  $\text{cm}^{-1}$  region. UV–visible spectra were recorded on a Shimadzu UV-2600 spectrometer. Steady-state fluorescence spectra were recorded on Hitachi F-4600 spectrophotometers. The pH of buffered solution was determined using a PHS-3C digital pH-meter (Leici, Shanghai, China).

### 2.3. Synthesis

The synthesis route of **V1** is shown in Scheme 1.

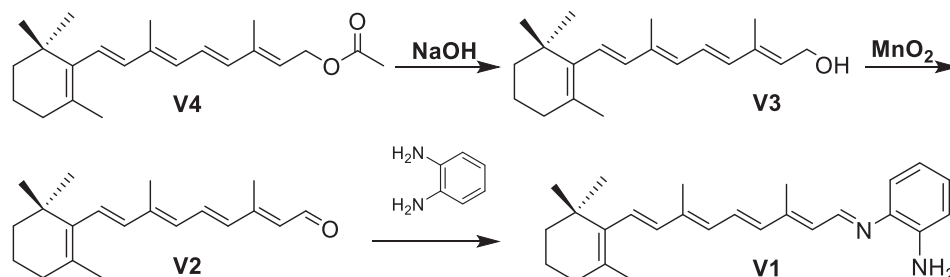
Synthesis of **V3**: The commercial retinol acetate **V4** (10.0 g) was dissolved in 75.0 mL NaOH solution (1 M) and 75.0 mL THF. Then the mixture is stirred at the room temperature for 12 h under nitrogen atmosphere. After the reaction finished, the reaction mixture was transferred to separating funnel, standing and separation of organic and aqueous phases. The aqueous phase was washed by THF and ethyl acetate three times. The organic layer was combined and dried by  $\text{Na}_2\text{SO}_4$ . The organic solvent was evaporated by rotary evaporator, obtaining 4.5 g light yellow oil, yield 60%. The crude product was used in the following reaction without purification [27].

Synthesis of **V2**: The retinol (2.1 g, 7.34 mmol) and  $\text{Na}_2\text{CO}_3$  (11.66 g, 0.11 mol) was dissolved in 130 mL THF and cooled to  $0^\circ\text{C}$  in ice bar. The  $\text{MnO}_2$  (9.57 g, 0.11 mol) was slowly added into above cooling mixture. The reaction mixture was continually stirred for 1 h after removing the ice bar. The reaction residue was separated by vacuum filtration, retaining filtrate [27]. The crude product was concentrated and further purified by silica gel column chromatography, obtaining light yellow waxy solid 0.6 g, yield 29%.  $^1\text{H}$  NMR (400 MHz,  $\text{CDCl}_3$ )  $\delta$  10.11 (d,  $J = 8.2$  Hz, 1H), 7.14 (dd,  $J = 15.1, 11.5$  Hz, 1H), 6.36 (dd,  $J = 15.5, 11.5$  Hz, 2H), 6.22–6.13 (m, 2H), 5.97 (d,  $J = 8.2$  Hz, 1H), 2.33 (d,  $J = 0.9$  Hz, 3H), 2.07–1.98 (m, 5H), 1.72 (s, 3H), 1.65–1.60 (m, 3H), 1.49–1.45 (m, 2H), 1.04 (s, 6H).

Synthesis of **V1**: The retinal (0.30 g, 1.06 mmol) and *o*-Phenylenediamine (0.34 g, 3.18 mmol) was refluxed in 35 mL acetonitrile for 2 h. The solvent was evaporated by rotary evaporator, getting crude product. The crude product was recrystallized in 20 mL petroleum ether and 2 mL ethanol [24], cooling and vacuum filtration, obtaining orange solid 0.35 g, yield 87.5%.  $^1\text{H}$  NMR (400 MHz,  $\text{DMSO-}d_6$ )  $\delta$  8.64 (d,  $J = 9.7$  Hz, 1H), 7.08 (dd,  $J = 8.0, 1.2$  Hz, 1H), 7.02–6.88 (m, 2H), 6.67 (dd,  $J = 8.0, 1.3$  Hz, 1H), 6.60–6.45 (m, 2H), 6.44–6.33 (m, 1H), 6.24 (dt,  $J = 29.7, 11.7$  Hz, 3H), 5.06 (s, 2H), 2.20 (s, 3H), 2.06–1.94 (m, 5H), 1.70 (s, 3H), 1.58 (dt,  $J = 8.5, 4.7$  Hz, 2H), 1.49–1.39 (m, 2H), 1.02 (s, 6H).  $^{13}\text{C}$  NMR (101 MHz,  $\text{CDCl}_3$ )  $\delta$  155.25, 154.42, 143.70, 137.63, 136.96, 135.45, 134.27, 131.43, 131.22, 129.85, 124.84, 114.79, 112.57, 79.28, 39.65, 34.33, 33.29, 29.02, 21.87, 19.17, 14.05, 13.18. HR-MS: calcd for  $\text{C}_{26}\text{H}_{36}\text{N}_2^+$  [ $\text{M}+\text{H}$ ] $^+$ , 375.2800; found: 375.2803.

### 2.4. Procedures of the metal ion sensing

The solutions of metal ions (10.0 mM) were prepared in doubly distilled water by the dissolution of their corresponding nitrate salts, including  $\text{Al}^{3+}$ ,  $\text{Ca}^{2+}$ ,  $\text{Cr}^{3+}$ ,  $\text{Mn}^{2+}$ ,  $\text{Fe}^{3+}$ ,  $\text{Be}^{2+}$ ,  $\text{Ni}^{2+}$ ,  $\text{Cu}^{2+}$ ,  $\text{Zn}^{2+}$ ,  $\text{Ag}^+$ ,  $\text{Cd}^{2+}$ ,  $\text{Ba}^{2+}$ ,  $\text{Hg}^{2+}$ ,  $\text{Pb}^{2+}$ ,  $\text{K}^+$ ,  $\text{Na}^+$ ,  $\text{Mg}^{2+}$ . Stock solution of **V1** ( $1.0 \times 10^{-3}$  mol/L) was prepared in acetonitrile or DMSO by dissolving the corresponding amount of **V1** powder and then diluted to  $1.0 \times 10^{-5}$  mol/L with acetonitrile, DMSO/stroke-physiological saline solution (1:1000, v/v; pH = 6.5). Human serum was added into the test solution according to the mass ratio. In titration experiments, test solution of **V1** (2 mL) was filled in a quartz optical cell of 1 cm optical path length, and then aliquots of 2  $\mu\text{L}$  of  $\text{Cu}(\text{NO}_3)_2$  solution ( $1.0 \times 10^{-2}$  mol/L) were gradually added by using a micro-pipette. Spectral data were recorded for 5 min after addition of the metal ions at steady temperature (298 K). For fluorescence measurements, the excitation wavelength was at 400 nm using Xe lamp as an excitation source, the fluorescence emission channel was from 410 to 800 nm. In pH titration experiments, stock solution of **V1** was added to the sodium phosphate buffer aqueous solution with different pH values. The **V1**– $\text{Cu}^{2+}$  complex preparation, 1.12 mg (3 mmol) **V1** and 0.6 mg (3.6 mmol)  $\text{Cu}(\text{NO}_3)_2$  was dissolved in 5 mL acetonitrile and stirred for 5 min, and then the



Scheme 1. Synthesis of compound **V1**.

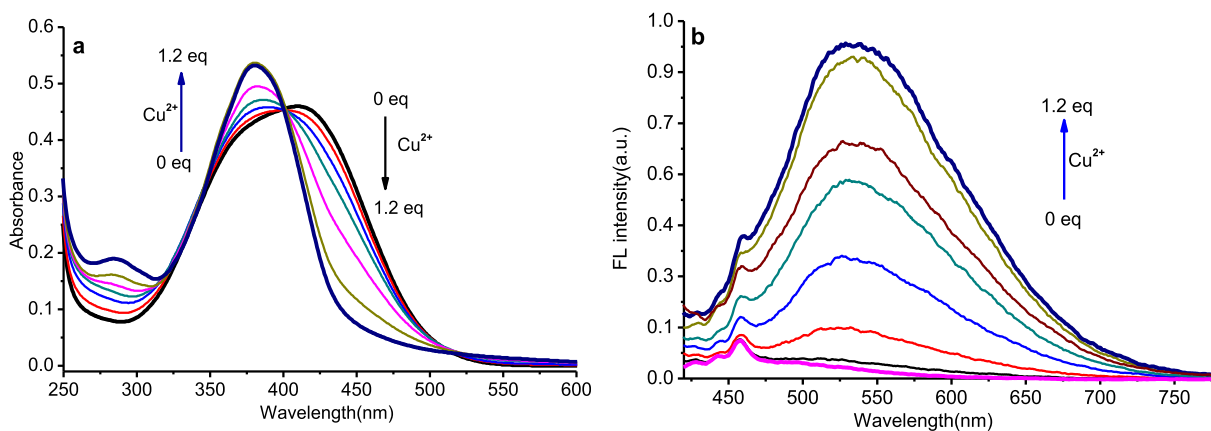


**Fig. 1.** Absorption spectra (a) and fluorescence spectra (b) of **V1** (10 μmol/L) with the addition of increasing concentrations of Cu<sup>2+</sup> (0–12 μmol/L) in acetonitrile (Ex = 400 nm).

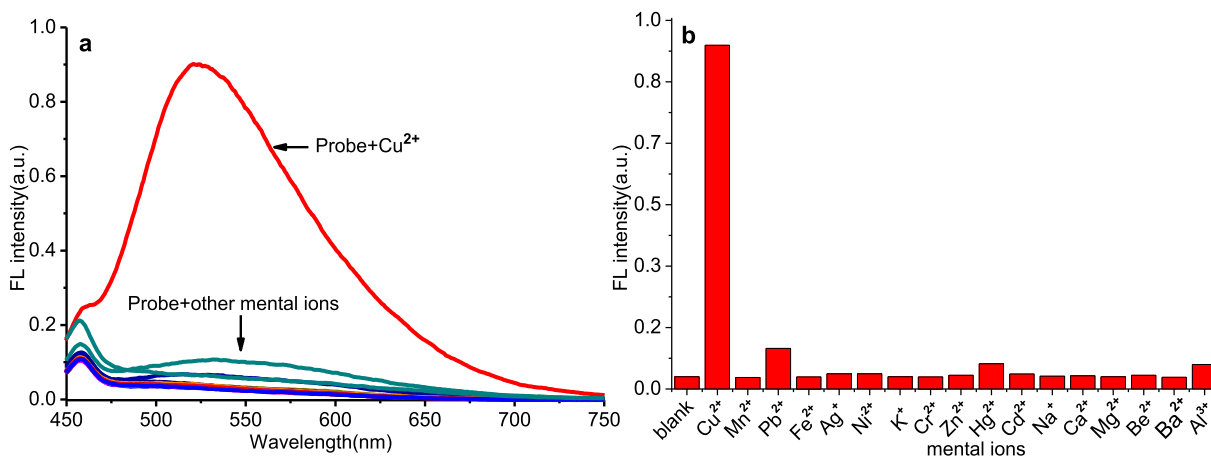


**Fig. 2.** The fluorescence spectra (a) and histogram (b) at 525 nm of probe **V1** (10 μmol/L) upon the addition of various metal ions (10 μmol/L) in the presence of Cu<sup>2+</sup> (10 μmol/L) as background in acetonitrile.

solvent was evaporated by rotary evaporator, getting powder product **V1**–Cu<sup>2+</sup> complex. The sample was used directly for infrared (FT-IR) spectra testing without purification.

### 3. Results and discussion

#### 3.1. Spectral characteristics

The absorption and fluorescence spectra of **V1** ( $1.0 \times 10^{-5}$  M) in acetonitrile was explored. As shown in Fig. 1a, there was a wide absorption band centered at 415 nm in the range 300–500 nm.

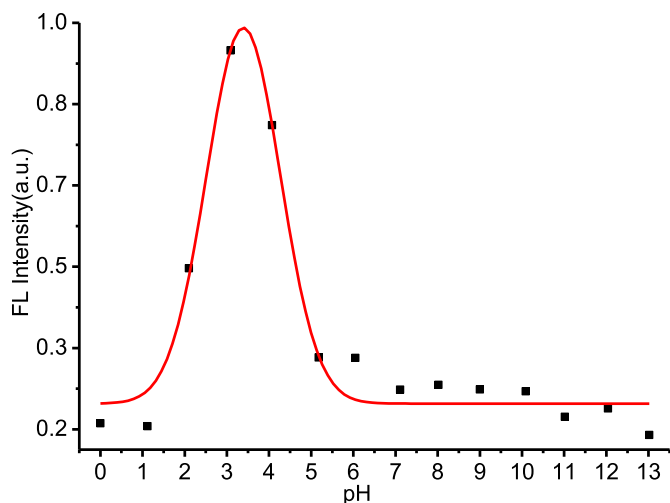


**Fig. 3.** The fluorescence intensity at 525 nm of probe **V1** (10 μM) in PBS solution at different pH values (λ<sub>ex</sub> = 380 nm).

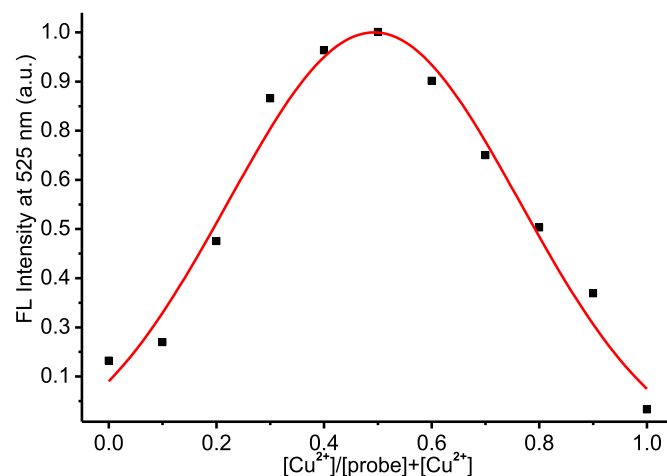


**Fig. 4.** Job's plot of the binding between probe and Cu<sup>2+</sup>. Fluorescence at 525 nm (λ<sub>ex</sub> = 380 nm) was plotted as a function of the molar ratio [Cu<sup>2+</sup>]/([probe]+[Cu<sup>2+</sup>]) (the total concentration of probe and Cu<sup>2+</sup> were 20 μmol/L).

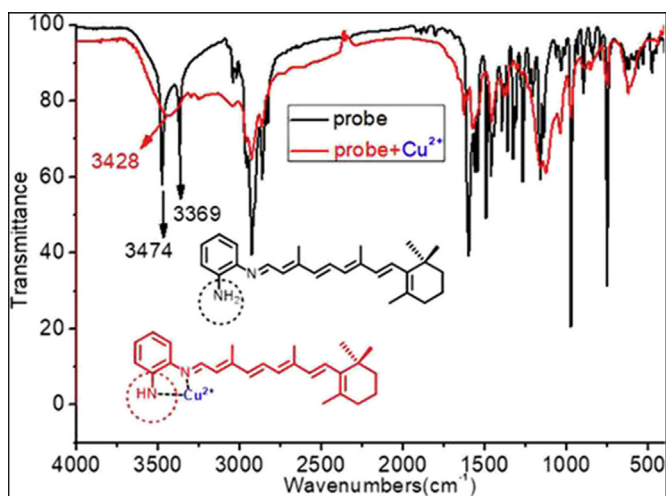
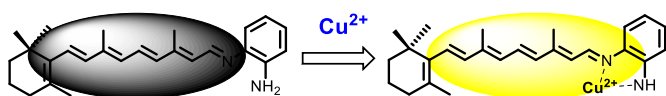


Fig. 5. Infrared spectra of compound **V1** (black) and **V1**- $\text{Cu}^{2+}$  (red).



Scheme 2. The proposed binding mechanism of compound **V1** with  $\text{Cu}^{2+}$ .

Under the excitation of 400 nm light, no fluorescence emission peak of **V1** was detected within 425–750 nm (Fig. 2b). And then, the quantitative copper ions were gradually added to **V1** solution. Correspondingly, the original absorption peak at 415 nm regularly blue shift to 380 nm. The isosbestic point at 400 nm indicated the existence of an equilibrium between **V1** and **V1**- $\text{Cu}^{2+}$  complex (Fig. 1a). The fluorescence emission peak at 525 nm gradually increased with the increasing concentrations of  $\text{Cu}^{2+}$ . After 1.2 equivalents of copper ions were added to the **V1** solution, the intensity of the fluorescence was significantly enhanced by 50 times (Fig. 1b). The change of UV–visible spectrum is attributed to the change of charge distribution of the probe due to the formation of complexes **V1**- $\text{Cu}^{2+}$ . The appearance of a fluorescent emission peak may involve the blocking of the photo-induced electron transfer when imine and amine groups coordinated to the copper ion [28].

### 3.2. Selectivity

As the recognition group, Schiff base structure has excellent selectivity to copper ion [24,28]. The fluorescent probe **V1** based on Schiff base structure of retinal and *o*-phenylenediamine inherit the

characteristics of excellent selectivity. The experimental data also demonstrates that the probe **V1** has a high selectivity for copper ions. After the 16 different metal ions ( $\text{Mn}^{2+}$ ,  $\text{pb}^{2+}$ ,  $\text{Fe}^{2+}$ ,  $\text{Ag}^+$ ,  $\text{Ni}^{2+}$ ,  $\text{K}^+$ ,  $\text{Cr}^{3+}$ ,  $\text{Zn}^{2+}$ ,  $\text{Hg}^{2+}$ ,  $\text{Cd}^{2+}$ ,  $\text{Na}^+$ ,  $\text{Ca}^{2+}$ ,  $\text{Mg}^{2+}$ ,  $\text{Be}^{2+}$ ,  $\text{Ba}^{2+}$  and  $\text{Al}^{3+}$ ) were separately added into **V1** solution, only slight changes were observed in its fluorescence spectra. The fluorescence enhancement process happened only in the presence of  $\text{Cu}^{2+}$  compared to the blank (Fig. 2). The corresponding absorption spectra changes of **V1** were shown in Fig. S5.

### 3.3. Effects of pH

The nitrogen-containing chelator is susceptible to acid-base effects [29,30]. Therefore, it is necessary to check the fluorescence properties of **V1** in solution at different pH values. The acid–base titration experiments were carried out by adjusting the pH with an aqueous solution of NaOH and HCl of phosphate-buffered saline (PBS) (Fig. 3). As evidenced in Fig. 5, these results showed that the fluorescence at 525 nm of free **V1** was low and varied little in a wide range (pH = 6.0–13.0). The probe showed the increased fluorescence intensity at 525 nm in the acidic medium (pH = 1.0–5.0). It can be predicted that probe **V1** could be used in drinking water and also sense the  $\text{Cu}^{2+}$  concentration under physiological conditions for biological applications. The proposed mechanism for the fluorescence of **V1** affected by pH may be that the protonated nitrogen atom inhibited the quenching process via the photo-induced electron transfer (PET) from *o*-phenylenediamino to the excited fluorophore retinal [31].

### 3.4. Sensing mechanism

Theoretically, probes and analytes have specific stoichiometric ratios, using coordination as sensing mechanism [32]. Therefore the binding stoichiometry between **V1** and  $\text{Cu}^{2+}$  was investigated through Job's plot experiments (Fig. 4). The fluorescence emission intensities of **V1** and  $\text{Cu}^{2+}$  mixture at 525 nm were recorded. The molar fraction of  $\text{Cu}^{2+}$  with a constant total concentration of **V1** and  $\text{Cu}^{2+}$  (20  $\mu\text{mol}$ ) varied from 0 to 1. The fluorescence emission intensities at 525 nm reached maximum value, when the molar fraction was 0.5 for **V1**, indicating the formation of 1 : 1 complexes between the **V1** and  $\text{Cu}^{2+}$  (Scheme 2).

To further explore the binding mechanism in detail, the infrared spectra of compound **V1** and its coordination complex **V1**- $\text{Cu}^{2+}$  were measured. The infrared spectrum of **V1** and **V1**- $\text{Cu}^{2+}$  were overlaid and compared (Fig. 5). The significant differences in spectra can lead to important inferences. Firstly, two N–H stretching vibration peaks of the N– $\text{H}_2$  group at  $3369\text{ cm}^{-1}$  and

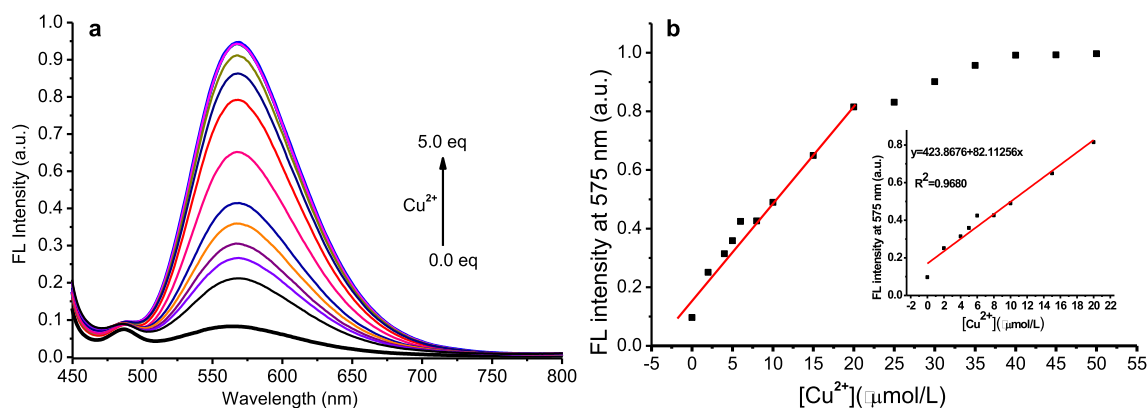
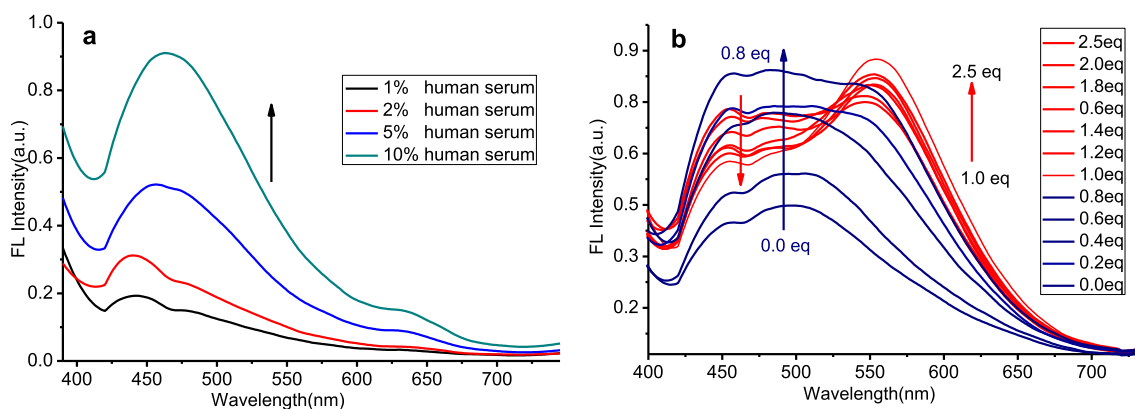


Fig. 6. (a) Fluorescence spectra of **V1** (10  $\mu\text{mol/L}$ ) with the addition of increasing concentrations of  $\text{Cu}^{2+}$  (0–50  $\mu\text{mol/L}$ ) in physiological saline (DMSO/physiological saline (V/V) = 1:1000, pH = 6.5, Ex = 400 nm). (b) The curves of the fluorescence emission intensity at 575 nm versus the concentration of  $\text{Cu}^{2+}$ . Inset: Calibration curve in the concentrations range of 0–20  $\mu\text{mol/L}$  of  $\text{Cu}^{2+}$ .



**Fig. 7.** (a) Fluorescence spectra of **V1** (10  $\mu\text{M}$ ) in the presence of different human serum solution (1%, 2%, 5%, 10% human serum); (b) Fluorescence spectra of **V1** (10  $\mu\text{M/L}$ ) with the addition of increasing concentrations of  $\text{Cu}^{2+}$  (0–25  $\mu\text{mol/L}$ ) in physiological saline containing 2% human serum ( $\lambda_{\text{exc}} = 380 \text{ nm}$ ).

$3474 \text{ cm}^{-1}$  was obvious recorded in the free **V1** molecular. Secondly, after the  $\text{N-H}_2$  group on phenylenediamino binding with  $\text{Cu}^{2+}$ , the two stretching vibration peaks of  $\text{N-H}_2$  group disappeared. Instead, the single stretching vibration of the  $\text{N-H}$  at  $3428 \text{ cm}^{-1}$  appeared in the coordination complex **V1**– $\text{Cu}^{2+}$  (Fig. 5). According to the Job's plot and infrared spectra, a proposed binding mechanism of **V1** with  $\text{Cu}^{2+}$  was shown in Scheme 2. Two nitrogen atoms on the phenylenediamino can cooperatively participate in the binding with  $\text{Cu}^{2+}$ .

### 3.5. Sensing of $\text{Cu}^{2+}$ in physiological saline and human serum

In order to assess the practical application of the probe **V1**, the titration experiment for  $\text{Cu}^{2+}$  were carried out in physiological saline (Fig. 6a). As shown in Fig. 6a, the emission intensity at 575 nm gradually increased with the increasing concentrations of  $\text{Cu}^{2+}$  until 50  $\mu\text{mol/L}$   $\text{Cu}^{2+}$ . Due to the strong polarity of physiological saline, the fluorescence emission of **V1** shifted from 525 nm (in acetonitrile) to 575 nm [33]. Furthermore, the curve of the fluorescence emission intensity at 575 nm versus the concentration of  $\text{Cu}^{2+}$  appeared a good linear relationship in the range of 0–20  $\mu\text{mol/L}$  of  $\text{Cu}^{2+}$  (Fig. 6b). The linear equation was  $y = 82.1125x + 423.8676$  ( $R^2 = 0.9680$ ) and the detection limit of **V1** for  $\text{Cu}^{2+}$  was 0.05  $\mu\text{mol/L}$  [34]. Therefore, the probe **V1** is fully capable of detecting copper ions in drinking water (ca. 20.0 mol/L) [35] or blood (ca. 15.7–23.6 mol/L) [36]. These basic experimental data will provide an important reference for the probe application in the actual physiological environment.

In order to give insight to the advantages of retinal compatibility with the protein environment, the titration experiment for  $\text{Cu}^{2+}$  were carried out in human serum solution. The residues of proteins in serum have strong chelation to copper ions and compete with probes. In addition, protein structure and probe interactions in serum may affect probe's fluorescence emission [37]. Both of these aspects will increase the difficulty of  $\text{Cu}^{2+}$  detection in serum solution. It was exciting that probe **V1** was able to differentially respond to serum proteins and copper ions, exhibiting different fluorescence emissions. As shown in Fig. 7a, owing to the slender conjugated polyene structure retinal of **V1** was conducive to entering protein structure, the emission intensity at 460 nm of **V1** gradually increased with the increasing concentrations of human serum. However, the fluorescence emission peaks at 460 nm and 550 nm both gradually increased in the range of 0–8  $\mu\text{mol/L}$  of  $\text{Cu}^{2+}$  in human serum (Fig. 7b). When the  $\text{Cu}^{2+}$  concentration from 10  $\mu\text{mol/L}$  increasing to 25  $\mu\text{mol/L}$ , the fluorescence emission peak at 460 nm gradually decreased and the peak at 550 nm continuously increased (Fig. 7b). Although most of the copper ions may be

sequestered by serum proteins in the low  $\text{Cu}^{2+}$  concentration range (0–8  $\mu\text{mol/L}$ ), the probe **V1** was still able to respond to chelated copper ions. This fully reflected the advantages of retinal chromophores in congenital compatibility with protein environment.

## 4. Conclusion

In summary, we have synthesized a novel retinal-based fluorescence probe **V1** that can be utilized as an excellent selectivity and sensitivity sensor for  $\text{Cu}^{2+}$ . This work opens up the use of flexible fluorophore retinal in fluorescent probes. In addition, the probe **V1** can work in physiological saline and serum which is important for possible use in a practical view on selective requirements for biomedical and environmental application. Further studies to develop fluorescent probe based on retinal are underway.

## Acknowledgements

This work was financially supported by Hubei Provincial Natural Science Foundation of China, China (Z2017105), Engineering Research Center of Eco-environment in Three Gorges Reservoir Region, China; Ministry of Education, China (KF2017-07), Research Foundation for High-level Talents of China Three Gorges University, China (1910103) and National Natural Science Foundation of China, China (21472111).

## Appendix A. Supplementary data

Supplementary data to this article can be found online at <https://doi.org/10.1016/j.saa.2019.117565>.

## References

- [1] J.L. Spudich, C.S. Yang, K.H. Jung, E.N. Spudich, Retinylidene proteins: structures and functions from archaea to humans, *Annu. Rev. Cell Dev. Biol.* (2000) 365–392.
- [2] G. Bassolino, T. Sovdat, A.S. Duarte, J.M. Lim, C. Schnedermann, M. Liebel, B. Odell, T.D.W. Claridge, S.P. Fletcher, P. Kukura, Barrier less photoisomerization of 11-cis retinal protonated Schiff base in solution, *J. Am. Chem. Soc.* 39 (2015) 12434–12437.
- [3] G. Bassolino, T. Sovdat, M. Liebel, C. Schnedermann, B. Odell, T.D.W. Claridge, P. Kukura, S.P. Fletcher, Synthetic control of retinal photochemistry and photophysics in solution, *J. Am. Chem. Soc.* 6 (2014) 2650–2658.
- [4] M. Liebel, P. Kukura, Lack of evidence for phase-only control of retinal photoisomerization in the strict one-photon limit, *Nat. Chem.* 1 (2017) 45–49.
- [5] T. Berbasova, M. Nosrati, C. Vasileiou, W. Wang, K. Sing, S. Lee, I. Yapiçi, J.H. Geiger, B. Borhan, Rational design of a colorimetric pH sensor from a soluble retinoic acid chaperone, *J. Am. Chem. Soc.* 43 (2013) 16111–16119.
- [6] A.J. Cruz, K. Siam, C. Moore, M. Islam, D.P. Rillema, Dicyano and pyridine derivatives of retinal: synthesis and vibronic, electronic, and photophysical properties, *J. Phys. Chem. A* 25 (2010) 6766–6775.

- [7] N.J. Robinson, D.R. Winge, in: R.D. Kornberg, C. Raetz, J.E. Rothman, J.W. Thorner (Eds.), *Annual Review of Biochemistry*, vol. 79, 2010, pp. 537–562 (Chapter).
- [8] C.J. Maynard, R. Cappai, I. Volitakis, R.A. Cherny, A.R. White, K. Beyreuther, C.L. Masters, A.I. Bush, Q.X. Li, Overexpression of Alzheimer's disease amyloid-beta opposes the age-dependent elevations of brain copper and iron, *J. Biol. Chem.* 277 (2002) 44670–44676.
- [9] J. Emerit, A. Edeas, F. Bricaire, Neurodegenerative diseases and oxidative stress, *Biomed. Pharmacother.* 1 (2004) 39–46.
- [10] K.J. Barnham, A.I. Bush, Metals in Alzheimer's and Parkinson's diseases, *Curr. Opin. Chem. Biol.* 2 (2008) 222–228.
- [11] G.L. Millhauser, Copper binding in the prion protein, *Accounts Chem. Res.* 2 (2004) 79–85.
- [12] G.J. Brewer, Copper in medicine, *Curr. Opin. Chem. Biol.* 2 (2003) 207–212.
- [13] L.I. Bruijn, T.M. Miller, D.W. Cleveland, Unraveling the mechanisms involved in motor neuron degeneration in ALS, *Annu. Rev. Neurosci.* (2004) 723–749.
- [14] K.C. Ko, J.S. Wu, H.J. Kim, P.S. Kwon, J.W. Kim, R.A. Bartsch, J.Y. Lee, J.S. Kim, Rationally designed fluorescence 'turn-on' sensor for  $\text{Cu}^{2+}$ , *Chem. Commun.* 11 (2011) 3165–3167.
- [15] S.P. Wu, T.H. Wang, S.R. Liu, A highly selective turn-on fluorescent chemosensor for copper(II) ion, *Tetrahedron* 51 (2010) 9655–9658.
- [16] R.L. Sheng, P.F. Wang, Y.H. Gao, Y. Wu, W.M. Liu, J.J. Ma, H.P. Li, S.K. Wu, Colorimetric test kit for  $\text{Cu}^{2+}$  detection, *Org. Lett.* 21 (2008) 5015–5018.
- [17] N.K. Singhal, B. Ramanujam, V. Mariappanadar, C.P. Rao, Carbohydrate-based switch-on molecular sensor for Cu(II) in buffer: absorption and fluorescence study of the selective recognition of Cu(II) ions by galactosyl derivatives in HEPES buffer, *Org. Lett.* 16 (2006) 3525–3528.
- [18] W. Lin, L. Yuan, W. Tan, J. Feng, L. Long, Construction of fluorescent probes via protection/deprotection of functional groups: a ratiometric fluorescent probe for  $\text{Cu}^{2+}$ , *Chem. Eur J.* 4 (2009) 1030–1035.
- [19] M. Yu, M. Shi, Z. Chen, F. Li, X. Li, Y. Gao, J. Xu, H. Yang, Z. Zhou, T. Yi, C. Huang, Highly sensitive and fast responsive fluorescence turn-on chemodosimeter for  $\text{Cu}^{2+}$  and its application in live cell imaging, *Chem. Eur J.* 23 (2008) 6892–6900.
- [20] L.A. Huang, F.J. Chen, P.X. Xi, G.Q. Xie, Z.P. Li, Y.J. Shi, M. Xu, H.Y. Liu, Z.R. Ma, D.C. Bai, Z.Z. Zeng, A turn-on fluorescent chemosensor for  $\text{Cu}^{2+}$  in aqueous media and its application to bioimaging, *Dyes Pigments* 3 (2011) 265–268.
- [21] Y. Zhao, X.B. Zhang, Z.X. Han, L. Qiao, C.Y. Li, L.X. Jian, G.L. Shen, R.Q. Yu, Highly sensitive and selective colorimetric and off-on fluorescent chemosensor for  $\text{Cu}^{2+}$  in aqueous solution and living cells, *Anal. Chem.* 16 (2009) 7022–7030.
- [22] Y. Xiang, A.J. Tong, P.Y. Jin, Y. Ju, New fluorescent rhodamine hydrazone chemosensor for Cu(II) with high selectivity and sensitivity, *Org. Lett.* 13 (2006) 2863–2866.
- [23] Y. Zhou, F. Wang, Y. Kim, S.J. Kim, J. Yoon,  $\text{Cu}^{2+}$ -Selective ratiometric and "Off-On" sensor based on the rhodamine derivative bearing pyrene group, *Org. Lett.* 19 (2009) 4442–4445.
- [24] H. Lan, B. Liu, G. Lv, Z. Li, X. Yu, K. Liu, X. Cao, H. Yang, S. Yang, T. Yi, Dual-channel fluorescence "turn on" probe for  $\text{Cu}^{2+}$ , *Sens. Actuators B Chem.* 0 (2012) 811–816.
- [25] P.J.M. Johnson, A. Halpin, T. Morizumi, V.I. Prokhorenko, O.P. Ernst, R.J.D. Miller, Local vibrational coherences drive the primary photochemistry of vision, *Nat. Chem.* 12 (2015) 980–986.
- [26] G. Bassolino, T. Sovdat, M. Liebel, C. Schnedermann, B. Odell, T.D.W. Claridge, P. Kukura, S.P. Fletcher, Synthetic control of retinal photochemistry and photophysics in solution, *J. Am. Chem. Soc.* 6 (2014) 2650–2658.
- [27] N. Font N, M. Dom Nguéz, R. Lvarez, N.R. de Lera, Synthesis of C40-symmetrical fully conjugated carotenoids by olefin metathesis, *Eur. J. Org. Chem.* 33 (2011) 6704–6712.
- [28] S.P. Wu, T.H. Wang, S.R. Liu, A highly selective turn-on fluorescent chemosensor for copper(II) ion, *Tetrahedron* 51 (2010) 9655–9658.
- [29] H. Lan, Y. Wen, Y. Shi, K. Liu, Y. Mao, T. Yi, Fluorescence turn-on detection of  $\text{Sn}^{2+}$  in live eukaryotic and prokaryotic cells, *Analyst* 20 (2014) 5223–5229.
- [30] L. Liu, F. Dan, W. Liu, X. Lu, Y. Han, S. Xiao, H. Lan, A high-contrast colorimetric and fluorescent probe for  $\text{Cu}^{2+}$  based on benzimidazole-quinoline, *Sens. Actuators B Chem.* (2017) 445–450.
- [31] Y. Sun, J. Liu, H. Zhang, Y. Huo, X. Lv, Y. Shi, W. Guo, A mitochondria-targetable fluorescent probe for dual-channel NO imaging assisted by intracellular cysteine and glutathione, *J. Am. Chem. Soc.* 36 (2014) 12520–12523.
- [32] H.S. Kumbhar, B.L. Gadilohar, G.S. Shankarling, A highly selective quinaldine-indole based spiropyran with intramolecular H-bonding for visual detection of Cu(II) ions, *Sens. Actuators B Chem.* (2016) 35–42.
- [33] S.S. Bag, M.K. Pradhan, R. Kundu, S. Jana, Highly solvatochromic fluorescent naphthalimides: design, synthesis, photophysical properties and fluorescence switch-on sensing of ct-DNA, *Bioorg. Med. Chem. Lett* 1 (2013) 96–101.
- [34] C. Yu, L. Chen, J. Zhang, J. Li, P. Liu, W. Wang, B. Yan, Off-On" based fluorescent chemosensor for  $\text{Cu}^{2+}$  in aqueous media and living cells, *Talanta* 3 (2011) 1627–1633.
- [35] The probe is fully capable of detecting copper ions in water or blood A. Prasanna de Silva, H.Q. Nimal Gunaratne, Jean-Louis Habib-Jiwan, Colin P. McCoy, Terence E. Rice, Jean-Philippe Soumillion, New fluorescent model compounds for the study of photoinduced electron transfer: the influence of amolecular electric field in the excited state, *Angew. Chem. Int. Ed.* 34 (16) (1995) 1728–1731.
- [36] P. Job, Studies on the formation of complex minerals in solution and on their stability, *Ann. Chim. France* (1928) 113–203.
- [37] Yang Zhou, Jiaying Yan, Nuonuo Zhang, Dejiang Li, Shuzhang Xiao, Kaibo Zheng, A ratiometric fluorescent probe for formaldehyde in aqueous solution, serum and air using aza-cope reaction, *Sens. Actuators B Chem.* 258 (2018) 156–162.